ACS Combinatorial Science

Research Article

pubs.acs.org/acscombsci

Discovery of Overcoating Metal Oxides on Photoelectrode for Water Splitting by Automated Screening

Rie Saito, Yugo Miseki, Wang Nini, and Kazuhiro Sayama*

National Institute of Advanced Industrial Science and Technology (AIST), Central 5, 1-1-1 Higashi, Tsukuba, Ibaraki, 305-8565 Japan

Supporting Information

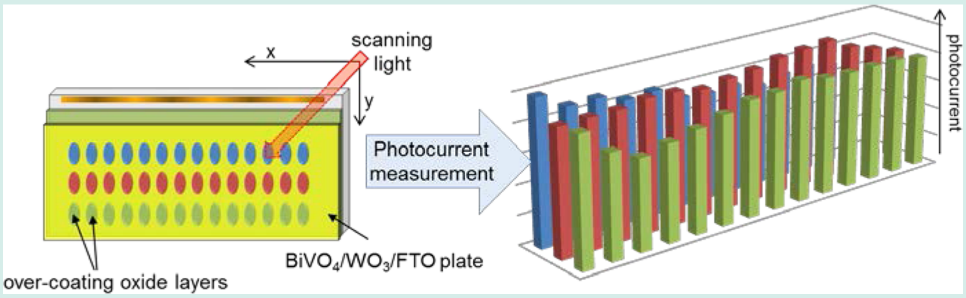

ABSTRACT: We applied an automated semiconductor synthesis and screen system to discover overcoating film materials and optimize coating conditions on the $BiVO_4/WO_3$ composite photoelectrode to enhance stability and photocurrent. Thirteen metallic elements for overcoating oxides were examined with various coating amounts. The stability of the $BiVO_4/WO_3$ photoelectrode in a highly concentrated carbonate electrolyte aqueous solution was significantly improved by overcoating with Ta_2O_5 film, which was amorphous and porous when calcined at 550 °C. The photocurrent for the water oxidation reaction was only minimally inhibited by the presence of the Ta_2O_5 film on the $BiVO_4/WO_3$ photoelectrode.

KEYWORDS: *photoelectrode library, composite multilayer, water splitting, metal oxides, automated screening, photocurrent*

INTRODUCTION

The development of renewable and nonpolluting energy resources is necessary to solve the energy and environmental problems caused by conventional fossil fuels. Hydrogen (H_2) production by the electrolysis of water using renewable energy sources is a highly desirable technology in this regard. While the thermodynamic water splitting voltage (ΔG) at 25 °C is 1.23 V, conventional water electrolysis requires an applied voltage of more than 1.6 V, representing a large overpotential for O_2 evolution. Significant reduction of the applied bias voltage can be accomplished by sunlight and various photoelectrodes of n-type semiconductors.[1−7] In this research field, porous oxide semiconductors, such as Fe_2O_3, $BiVO_4$, and WO_3, on a conducting glass electrode have shown high photocurrents under visible light. However, their solar energy conversion efficiencies have been insufficient for practical use. To utilize sunlight effectively, photoelectrodes with high conversion efficiency must be discovered and developed. Since our first report on the $BiVO_4$ photoelectrode,[8] this semiconductor has been intensively investigated for water splitting because of its suitable band potentials and high solar energy conversion efficiency.[5] In addition, we have reported the photocurrent behavior of $BiVO_4$ composite multilayer ($BiVO_4/WO_3$ under layer) electrodes in various electrolyte solutions.[9−12] In the phosphate, sulfate and carbonate electrolyte solutions, the best photocurrent behavior was obtained by the bicarbonate ion (HCO_3^-) electrolyte and it improved with increasing bicarbonate (HCO_3^-) electrolyte concentration, and very high applied bias photon-to-current efficiency (ABPE) > 1.35% could be obtained.[10,12] Moreover, the precise quantitative determination of evolved gases from water splitting showed the evolution of H_2 and O_2 in the stoichiometric ratio with the faradic efficiency of 100%. However, the stability of these $BiVO_4$ composite photoelectrodes has not yet been investigated in detail.

Several studies have reported that overcoating is a promising method to improve the stability of photoelectrodes.[13−16] However, the photooxidation reaction at the $BiVO_4$/electrolyte interface may be also inhibited by overcoating on the $BiVO_4$ surface, which would lead to a decrease in photocurrent. A search for optimal overcoating conditions involves various factors, such as overcoated film element, quantity, and film preparation temperature, giving rise to an enormous number of potential combinations. To accelerate the screening of the overcoating film conditions that provide an adequate photocurrent and stability, synthesis and evaluation procedures should be automated and accelerated.

We have developed two high-throughput screening systems for new visible-light responsive semiconductors for photoelectrodes. One is an automated synthesis system for a

Received: February 3, 2015
Revised: August 25, 2015
Published: September 1, 2015

DOI: 10.1021/acscombsci.5b00022
ACS Comb. Sci. 2015, 17, 592−599

photoelectrode library (array of semiconductor film samples) using the metal organic decomposition (MOD) method, and the other is a photocurrent evaluation system on a photoelectrode library.[17] Using these systems, we have developed several promising new materials, such as iron-based binary and iron/titanium-based ternary oxides, for n-type semiconductors and/or p-type semiconductors.[17,18]

We describe here the application of a similar search method and evaluation system to discover overcoating film materials and detect the optimal coating condition on the $BiVO_4/WO_3$ composite photoelectrode with high stability in bicarbonate ion electrolyte. We found that the stability of the $BiVO_4/WO_3$ photoelectrode in the highly concentrated carbonate electrolyte aqueous solution was significantly improved by overcoating with amorphous tantalum oxide film.

■ EXPERIMENTAL PROCEDURES

Preparation of the Photoelectrodes for Combinatorial Screening. The photoelectrode library was prepared using a wet-coating process as shown in Figure 1. Precursor solutions of various semiconductors were coated on a FTO (F-doped tin oxide) conductive glass plate (114 mm × 32 mm × 1 mm) and then calcined for each coating for 30 min under air. The FTO glass plates were made by Asahi Glass Co., Ltd. The detailed production method for the large $BiVO_4/WO_3$/FTO follows the method described in previous papers on small photoelectrodes.[10,11] In the automated synthesis, the precursor solution of various oxide semiconductors were MOD (metal organic decomposition) coating reagents obtained from Symetrix Co., USA. The detailed preparation method for concentration adjustment follows previous papers.[17,18] WO_3 and $BiVO_4$ films were coated over the entire area of the FTO conducting surface. First, a precursor solution of WO_3 was coated on FTO conductive glass using a spin coater at 1000 rpm and then calcined at 500 °C. Next, a precursor solution of $BiVO_4$ was coated using a spin coater at 1000 rpm and then calcined at 550 °C. This process was repeated twice. Then, the overcoating oxide films (4 mm × 8 mm) were coated in lines on the large $BiVO_4/WO_3$/FTO plate by using an automated synthesis system, as shown in Figure 1B. The precursor solution of various oxide samples was dropped on a $BiVO_4$ layer. The dropped solution was spread using a disposable tip moving, and excess solution was suctioned. Next, it was calcined at 550 °C. This process was repeated twice. Thirteen different metals were used for the overcoating oxide (Ta, Ti, Nb, Zn, La, In, Co, Fe, Sn, Zr, Mn, Si, and Mg). The formulas of the stable oxides are as follows: Ta_2O_5, TiO_2, Nb_2O_5, ZnO, La_2O_3, In_2O_3, CoO, Fe_2O_3, SnO_2, ZrO_2, MnO_2, SiO_2, and MgO. We selected these metal oxides which are relatively stable in the electrolyte solution, and which are formed by calcination using commercially available metal complex solutions for MOD from Symetrix Co.. Moreover, we mainly selected n-type semiconductor metal oxides. Because it is generally known that hole in n-type semiconductor is useful for the water oxidation to O_2, and that the photoelectrochemical properties could be improved by the formation of n-n junction such as $BiVO_4/WO_3$ and $BiVO_4/SnO_2$.

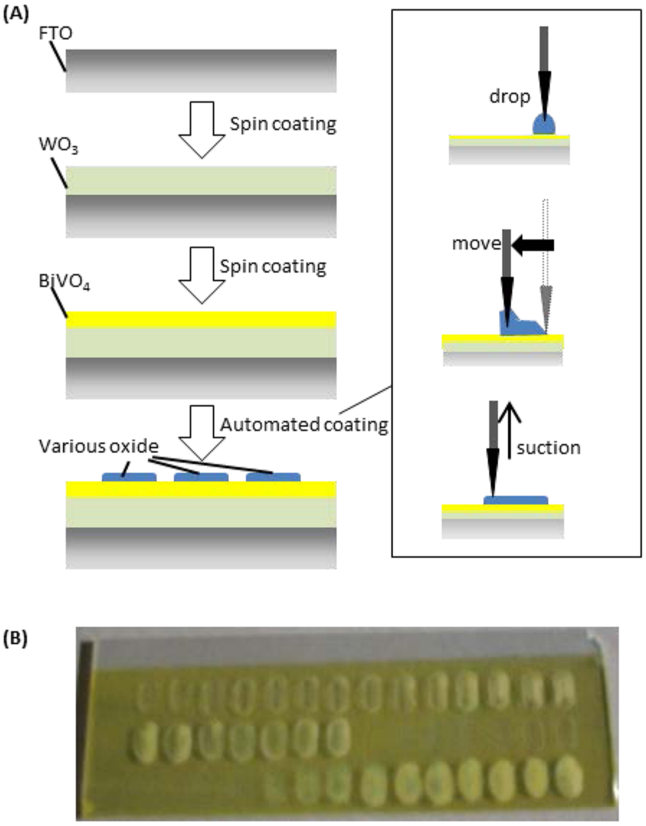

Figure 1. Preparation method (A) and a photograph (B) of the $BiVO_4/WO_3$ photoelectrode overcoated with metal oxides for combinatorial screening.

The doping effect of various metals (M) into the $BiVO_4$ film was also investigated to improve stability. The samples of M-doped $BiVO_4/WO_3$ were prepared using the same automated semiconductor synthesis system. Thirteen types of MOD solutions (Ta, Ti, Nb, Zn, La, In, Co, Fe, Sn, Zr, Mn, Si, and Mg) were added to the precursor solution of $BiVO_4$ (additive concentration: 20−0.25 mol %), and the solutions were mixed well by pipetting, and then they were coated on large WO_3/FTO plates.

Photoelectrochemical Measurements for Combinatorial Screening. The photoelectrochemical properties were investigated using a three-electrode system. This measurement condition is shown in Scheme 1a. The three electrodes were soaked in an electrolyte aqueous solution containing $KHCO_3$ (0.1 or 2.5 M). The current of photoelectrode was measured using an electrochemical analyzer (potentiostat, PS-08, Toho Technical Research Co., Ltd.) and a Pyrex glass cell. The working electrode was a photoelectrode, the reference electrode was Ag/AgCl, and the counter electrode was Pt wire. A copper foil was taped on the top of the photoelectrode to connect the cables to the working electrode. A xenon lamp (300 W, USHIO Inc.) equipped with an optical fiber and a 420 nm cutoff filter (HOYA, L-42) was used as the light source. The edge of the optical fiber was covered with a 1 mm hole slit. The on/off cycle of the light was repeated using a shutter. The optical fiber that was fixed to the *X*−*Y* stage was moved at constant speed to pass through the samples. The photocurrent was evaluated by measuring the current difference between when the light on the sample was turned on and off while applying a constant potential. For the stability acceleration experiment, the photoelectrode was soaked in the highly concentrated bicarbonate (2.5 M $KHCO_3$) electrolyte for a given length of time under the light irradiation, as shown in Scheme 1b. Subsequently, its photocurrent was measured again. The stability of the photoelectrode that was soaked in a 2.5 M

Scheme 1. Illustration of the Photoelectrochemical Measurements for Combinatorial Screening in the Stability Acceleration Experiments[a]

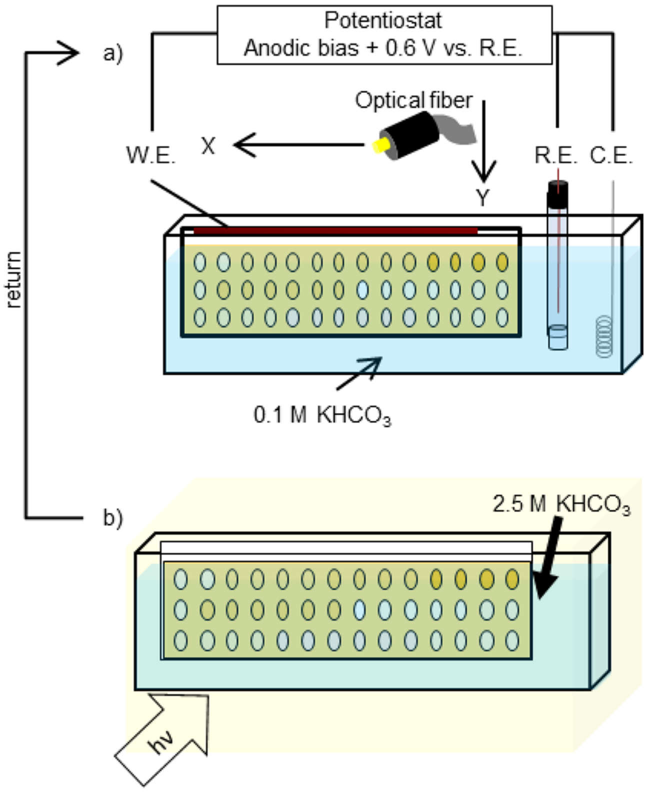

[a] (a) Measurement of the photocurrent in 0.1 M $KHCO_3$. (b) Dipping of the photoelectrode in 2.5 M $KHCO_3$ for 1 h.

carbonate electrolyte aqueous solution was evaluated using these photocurrents (Scheme 1). We confirmed that approximately the same photocurrent values were provided at any position of the $BiVO_4/WO_3$/FTO plate (Figure S1).

Electrochemical Characterization of the Selected Photoelectrode. The detailed photoelectrochemical properties were investigated as follows. The photoelectrode was prepared manually, and photocurrent−time-dependent change measurements of the electrode under a solar simulator (SAN-EI Electric Co., Ltd.) light irradiation were performed using an electrochemical analyzer (BAS Inc., ALS660B). The light with an intensity of 100 mW/cm^2 (AM 1.5) was irradiated to the glass plate of FTO. The photoelectrode area was 2 cm × 2.1 cm. Moreover, the multicomposite semiconductor thin film was characterized using a scanning electron microscope (SEM, Hitachi S-800, SE mode), X-ray fluorescence spectrometer (XRF, Rigaku ZSXmini), and X-ray diffractometer (PANalytical Empyrean).

RESULTS AND DISCUSSION

Typical Characterization of the $BiVO_4/WO_3$ Photoelectrode in Bicarbonate Aqueous Solution. The distinctive time-dependent change of photocurrent on the $BiVO_4/WO_3$ photoelectrode at +1.2 V_{RHE} is shown in Figure 2. The initial photocurrent in 2.5 M $KHCO_3$ aqueous solution increased approximately 1.4 times compared with that in 0.1 M. The photocurrent decreased significantly with increased irradiation time in 2.5 M $KHCO_3$ aqueous solution, and it was stable in 0.1 M. The turnover numbers (TONs) of electrons that flowed through the circuit to the $BiVO_4$ unit (mole number) in 0.1 and 2.5 M $KHCO_3$ aqueous solution for 1 h were approximately 652 and 380, respectively. These large TONs more than one indicate that a catalytic reaction progressed both in 0.1 and 2.5 M $KHCO_3$ aqueous solution. Figure 3 shows the amount of V, Bi, and W on the photoelectrode analyzed using XRF after the photoanodic reaction for 1 h. In 2.5 M $KHCO_3$ aqueous solution, the amounts of $BiVO_4$ film and WO_3 film were reduced by 100% and about 35% in 1 h, respectively, while the a decrease of the element amount was scarcely observed in 0.1 M $KHCO_3$ aqueous solution. In addition, in the photoelectrode with only the $BiVO_4$ film, the film was completely dissolved in 2.5 M $KHCO_3$ aqueous solution. It is obvious that the $BiVO_4$ was dissolved in the highly concentrated $KHCO_3$. This dissolution of the $BiVO_4/WO_3$ thin film leads to a decrease in the photocurrent. It was considered that not only the water oxidation reaction occurred on the $BiVO_4/WO_3$ film, but also the dissolution of the $BiVO_4/WO_3$ film in highly- concentrated $KHCO_3$ aqueous solution concurrently occurred gradually. Therefore, in this study on the photoelectrode stability, we used the highly concentrated $KHCO_3$ aqueous solution (2.5 M), because the initial photocurrent is high and suitable for an accelerated examination of the photoelectrode stability.

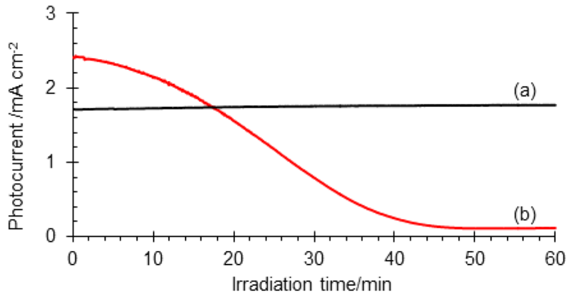

Figure 2. Time course of the photocurrent density of the $BiVO_4/WO_3$ photoelectrode in (a) 0.1 M and (b) 2.5 M KHCO3 aq. solution by stirring and CO_2 bubbling at +1.2 V vs RHE. Light source: Solar simulator AM 1.5. The direction of irradiation was to the FTO glass. The photoelectrode were prepared using a spin coater.

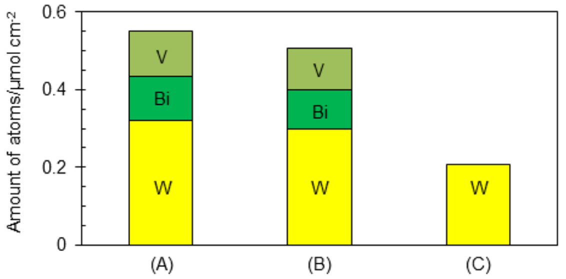

Figure 3. Changes before and after photoanodic reaction at +1.2 V vs RHE of the amount of elements on the $BiVO_4/WO_3$ photoelectrode: (A) before, (B) after 1 h in 0.1 M $KHCO_3$, and (C) after 1 h in 2.5 M $KHCO_3$: yellow, W; green, Bi; olive, V. Photoelectrodes were prepared using a spin coater.

Automated Screening of Overcoating Oxide Films. In the case of overcoating by metal oxide films on the $BiVO_4$ surface for protection against the dissolution of the photoanode, it is important that the initial photocurrent is not greatly decreased by the overcoating film. The synthesis and search for effective coating materials were performed by applying the automated screening system. The MOD stock solutions that

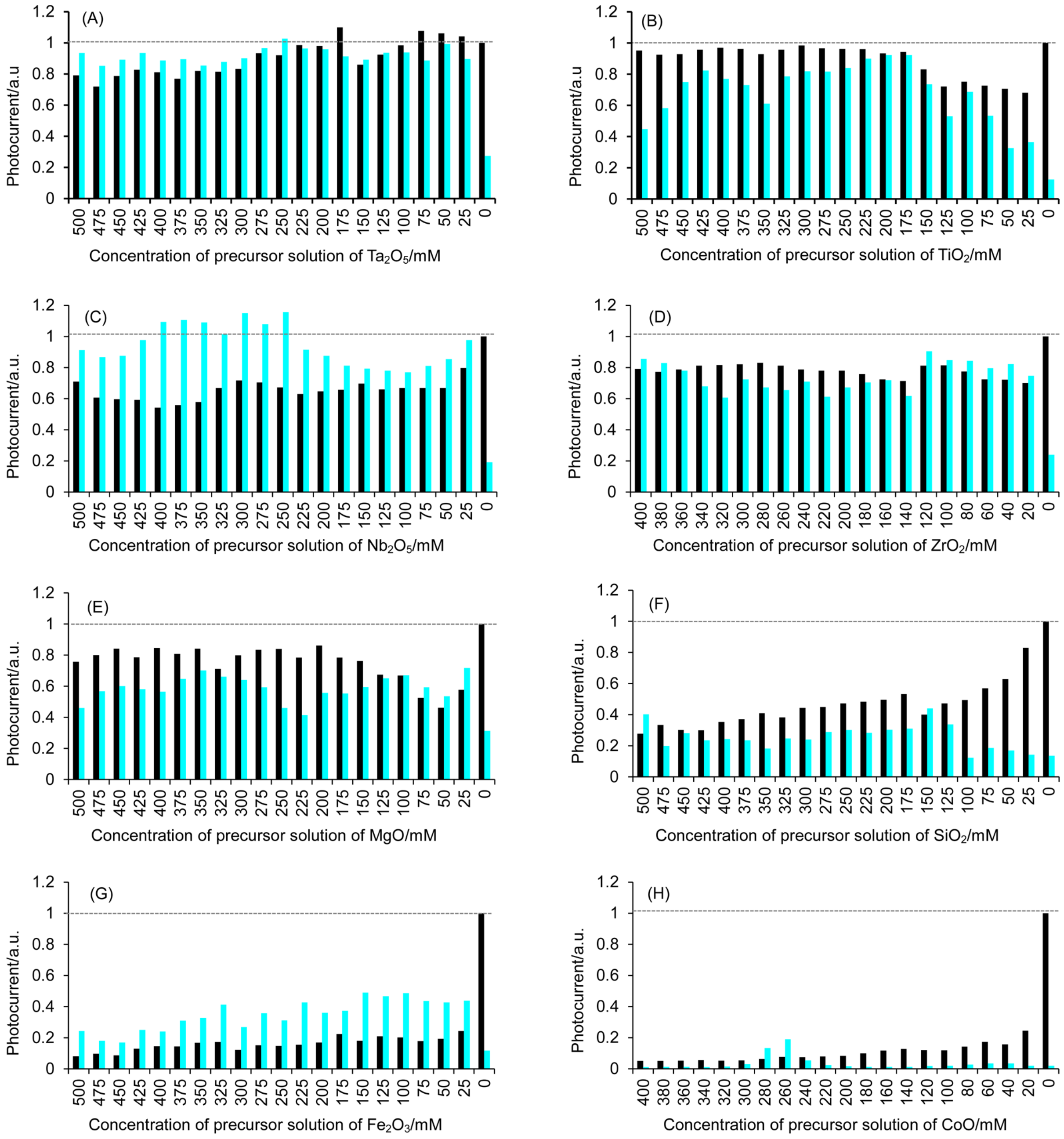

Figure 4. A comparative evaluation of the photocurrent of the multicomposite film samples. The samples were Ta_2O_5 (A), TiO_2 (B), Nb_2O_5 (C), ZrO_2 (D), MgO (E), SiO_2 (F), Fe_2O_3 (G), and CoO (H) coated on the $BiVO_4/WO_3$ electrode using the automated synthesis and screening system. Symbols: black, at start; blue, after 1 h.

were precursor solutions of various oxides were diluted every 5%. The amount of overcoated oxide films was adjusted by the concentration of the precursor solution.

First, the calcination temperature for overcoating oxide films was investigated at 550, 600, and 650 °C. In all cases, the photocurrents at over 600 °C were lower than those at 550 °C, regardless of the amount of coating oxidation products. Therefore, the optimum calcination temperature was found to be 550 °C. The photocurrents of $BiVO_4/WO_3$ photoelectrodes overcoated with various oxides were compared with those of the bare $BiVO_4/WO_3$ photoelectrode, as shown in Figure 4 and Figure S2. The 0 mM of the horizontal axis indicates the photocurrent without overcoating films on $BiVO_4/WO_3$ (i.e., bare $BiVO_4/WO_3$). The initial photocurrent of the bare $BiVO_4/WO_3$ photoanode was taken as a standard (initial photocurrent = 1 au), and the photocurrents at the start and after 1 h were compared. They were classified into 8 patterns. (1) Ta_2O_5: The decrease ratio of the initial photocurrent after Ta_2O_5 film coating was less than 20%. The photocurrent was minimally decreased, particularly in the low concentration range of precursor solution. These photocurrents were maintained for 1 h in a wide concentration range of precursor solution. (2)TiO_2: The decrease ratio of the initial photocurrent after coating was small in the high concentration range for overcoating solutions. A suitable amount of TiO_2 was necessary to maintain photocurrent value for 1 h. (3) Nb_2O_5: The decrease ratio of the initial photocurrent after coating was 40% regardless of the coating quantity, and it increased after 1

h. (4) ZrO_2 and SnO_2: The decrease ratio of the initial photocurrent after coating was below 40% regardless of coating quantity, and the photocurrent values were mostly maintained for 1 h. (5) MgO and In_2O_3: The decrease ratio of the initial photocurrent after coating was below 40% regardless of the coating quantity, and the photocurrent values were further decreased after 1 h. (6) SiO_2 and ZnO: The decrease ratio of the initial photocurrent after coating increased with increasing coating quantity, and the photocurrent values were further decreased after 1 h. (7) Fe_2O_3: The initial photocurrent was decreased by more than 80% by the coating. (8) La_2O_3, CoO, and MnO_2: The initial photocurrent value was decreased substantially after coating, even when the concentration of the precursor solution was below 20 mM.

It was found from the above results that photostability was enhanced by the Ta_2O_5, TiO_2, and Nb_2O_5 film overcoating. In the case of a precursor solution of 250 mM for the overcoating of metal oxide, the amounts of each oxide film, $BiVO_4$ and WO_3, after photoreaction for 1 h were analyzed using XRF, as shown in Table 1. The WO_3 film was perfectly protected against dissolution by overcoating in all three samples. The dissolution of the $BiVO_4$ film was also protected significantly by Ta_2O_5 coating. The decrease ratio of $BiVO_4$ film in the cases of TiO_2 and Nb_2O_5 coating was about 50% and 14%, respectively. The Ta_2O_5 coating was effective in ensuring the stability of the amount of $BiVO_4/WO_3$ film as well as the stability of the initial photocurrent and after 1 h.

Table 1. Variations of Each Layers after 1 h[a]

	decrease ratio (%) of various compounds		
sample	top layer (various covering layer)	$BiVO_4$	WO_3
$Ta_2O_5/BiVO_4/WO_3$	9	0	0
$TiO_2/BiVO_4/WO_3$	35	50	0
$Nb_2O_5/BiVO_4/WO_3$	25	14	0

[a] The photoelectrodes were prepared using the automated synthesis system.

Next, to improve the photoanode stability using another method, we also investigated the doping effect of various metals (M) into the $BiVO_4$ film. The 13 types (Ti−Mg) of MOD solutions were added to the precursor solution of $BiVO_4$, and then it was coated on WO_3 film. 550 °C was the optimum calcination temperature for the photocurrent for M-doped $BiVO_4/WO_3$ samples. The results for Ta-, Ti-, and Nb-doped $BiVO_4/WO_3$ at a calcination temperature of 550 °C are shown in Figure 5. The photocurrent values of various samples were measured with reference to the initial photocurrent of the nondoped sample. The initial photocurrents depended on the doping amounts and elements, and they decreased with increasing amounts of doped element. The photocurrents after photoreaction for 1 h were greatly decreased in all cases. Therefore, no clear improvement in the stability of the $BiVO_4/WO_3$ photoelectrode was observed using the doping method for 13 metallic elements into $BiVO_4$. In conclusion, using the automated screening method, we found that overcoating with Ta_2O_5 on the $BiVO_4/WO_3$ photoelectrode was better than that with other coating oxides and much better than the doping method.

Photoelectrochemical Stability of Overcoated Photoelectrode Prepared by Hand. We compared the results of the stability by using the automated screening system with that using a handmade preparation. The photoelectrode was prepared manually for a detailed characterization of the composite films ($Ta_2O_5/BiVO_4/WO_3$, $Nb_2O_5/BiVO_4/WO_3$, and $TiO_2/BiVO_4/WO_3$). The precursor solutions of these overcoating films were applied to a $BiVO_4/WO_3$/FTO using a spin coater, and the film was calcined at 550 °C in air for 30 min.

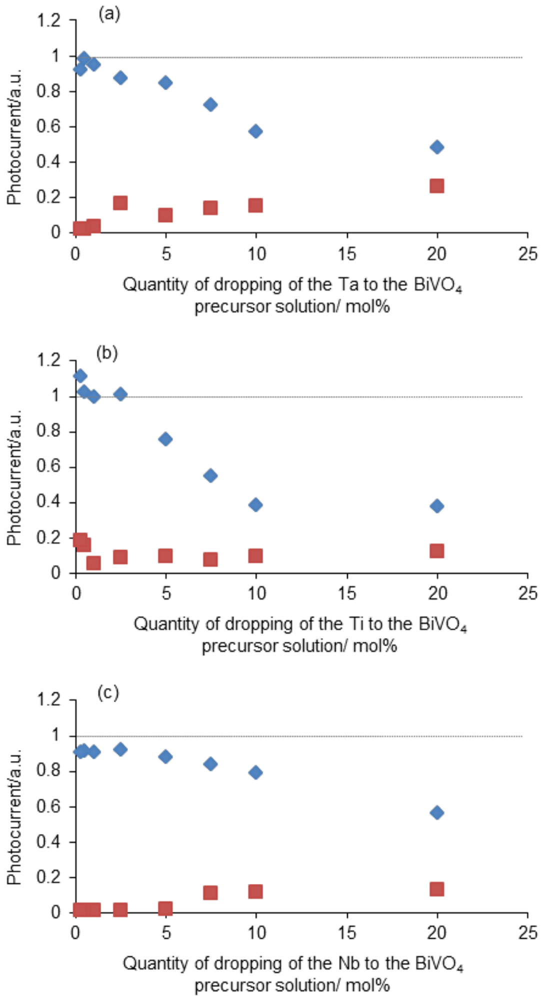

Figure 5. A comparative evaluation of the photocurrent of the M ((a) Ta, (b) Ti, and (c) Nb)-doped $BiVO_4/WO_3$ composite film samples:blue diamond, at start; red square, after 1 h. Photoelectrodes were prepared using the automated synthesis and screening system.

The photocurrent at +1.2 V_{RHE} was measured under solar simulator light irradiation for 200 min. The amounts of elements in the photoelectrodes obtained using XRF are shown in Figure 6. In the case of TiO_2 and Nb_2O_5 coatings, the $BiVO_4$ layer was completely dissolved within 100 and 200 min, respectively. In contrast, in the case of Ta_2O_5 coating (0.17 μmol cm^{-2}), it was found that the dissolution of the $BiVO_4$ layer was clearly inhibited. Therefore, the Ta_2O_5 overcoating was found to be the most effective in the inhibition of the dissolution of the $BiVO_4/WO_3$ photoelectrode in the case of the handmade preparation as well as the automated screening system. The photocurrent behavior of the $Ta_2O_5/BiVO_4/WO_3$ photoelectrode is shown in Figure 7. It was optimized in Ta_2O_5 film for stability and photocurrent. The photocurrent of the $Ta_2O_5/BiVO_4/WO_3$ photoelectrode did not decrease within 200 min, and that without Ta_2O_5 decreased gradually. The TON of electron to $BiVO_4$ of the $Ta_2O_5/BiVO_4/WO_3$

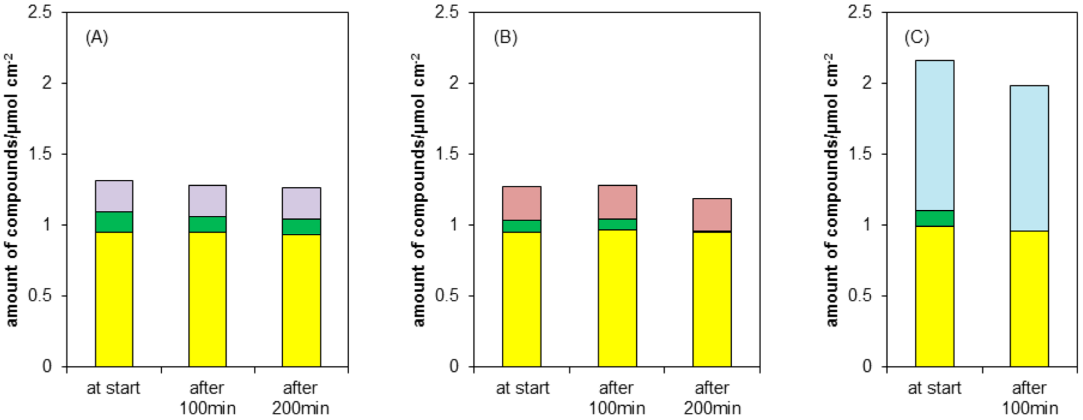

Figure 6. Changes before and after the photoanodic reaction in 2.5 M $KHCO_3$ at +1.2 V vs RHE of the amount of elements on the (A) Ta_2O_5/$BiVO_4$/WO_3, (B) Nb_2O_5/$BiVO_4$/WO_3, and (C) TiO_2/$BiVO_4$/WO_3 photoelectrodes: yellow, WO_3; green, $BiVO_4$; lilac, Ta_2O_5; pink, Nb_2O_5; blue, TiO_2. The photoelectrodes were prepared using a spin coater.

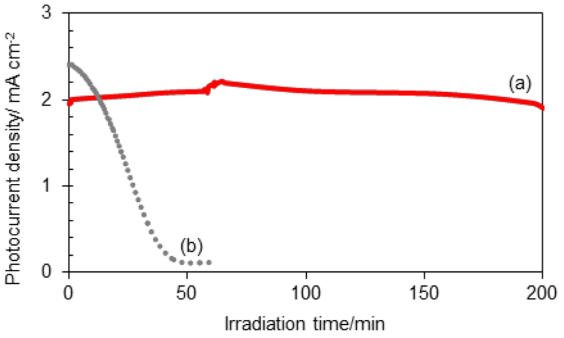

Figure 7. Time course of the photocurrent density of the (a) Ta_2O_5 (0.17 μmol cm^{-2})/$BiVO_4$/WO_3 and (b) $BiVO_4$/WO_3 photoelectrode in 2.5 M $KHCO_3$ aq. soln. with stirring and CO_2 bubbling at +1.2 V vs RHE. The photoelectrodes were prepared using a spin coater.

photoelectrode for 200 min was 1633 times, which was higher than that of the bare $BiVO_4$/WO_3 photoelectrode in Figure 2. It is suggested that the stability of the photocurrent was dominantly improved by Ta_2O_5 coating compared to the bare $BiVO_4$/WO_3 photoelectrode.

Role of the Overcoated Ta_2O_5 on the Enhancement of Photostability. Any peaks of Ta_2O_5 did not appear at 550 °C in the XRD pattern of the Ta_2O_5/$BiVO_4$/WO_3 film, suggesting that the Ta_2O_5 film of this sample was not a crystal (Figure S3). We prepared the Ta_2O_5 powder by the calcination of the same precursor solution used for the overcoated film. It was found that the XRD peaks of Ta_2O_5 were observed at 750 °C. The crystallization temperature of Ta_2O_5 is reported to be above 700 °C.[19] Therefore, it is expected that the Ta_2O_5 overcoating film existed as an amorphous, because the sample was prepared at a calcination temperature of 550 °C. Figure 8 shows the SEM images of the surface of the multicomposite photoelectrodes before and after coating with Ta_2O_5 film. The $BiVO_4$ particle size was 200−300 nm, and many pores between the $BiVO_4$ particles were observed before the Ta_2O_5 coating. It was clearly confirmed that the rough surface of $BiVO_4$ was completely covered by the Ta_2O_5 film as the amount of Ta_2O_5 analyzed by XRF increased. In the case of Ta_2O_5 (0.17 μmol cm^{-2})/$BiVO_4$/WO_3 in Figure 8 (A), in which the Ta_2O_5 film was optimized as shown in Figure 7, the surface of the Ta_2O_5 film was smooth and the particle shape of Ta_2O_5 film was not confirmed. The average thickness of this Ta_2O_5 film was calculated to be ∼90 nm using the amount of Ta_2O_5 with the theoretical density. The light absorption of this Ta_2O_5 film at >300 nm was negligible because of the large band gap, >4 eV, indicating that the Ta_2O_5 film did not prevent the absorption of light by $BiVO_4$/WO_3.

It is noteworthy that the decrease of the photocurrent by Ta_2O_5 overcoating was very little despite the existence of Ta_2O_5 film over the $BiVO_4$ surface. It is suggested that water oxidation was not inhibited by the Ta_2O_5 film. The top edge of the valence band of the crystalline $BiVO_4$ and Ta_2O_5 is about +2.5

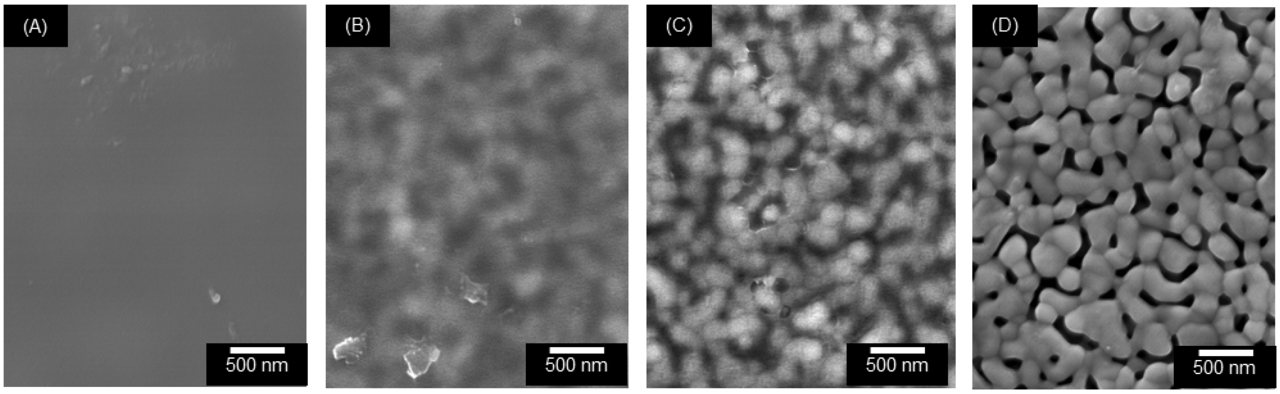

Figure 8. Surface SEM images of (A) Ta_2O_5 (0.17 μmol cm^{-2})/$BiVO_4$/WO_3, (B) Ta_2O_5 (0.13 μmol cm^{-2})/$BiVO_4$/WO_3, (C) Ta_2O_5 (0.046 μmol cm^{-2})/$BiVO_4$/WO_3, and (D) $BiVO_4$/WO_3. The photoelectrodes were prepared using a spin coater.

V (vs NHE pH = 0)[20] and +4.0 V,[21] respectively. The valence band potential of the amorphous Ta_2O_5 is not clear, but it might be difficult to explain the mechanism by the hole transfer from the $BiVO_4$ to water through the valence band of thick Ta_2O_5 layer with highly positive potential.

Figure S4 shows water oxidation over RuO_2/FTO and Ta_2O_5/RuO_2/FTO anodes without irradiation. RuO_2 is known to have a low overpotential for O_2 evolution (i.e., water oxidation) in the electrolysis of water.[22] The Ta_2O_5 film on the RuO_2/FTO was prepared using the same conditions as those for the $BiVO_4$/WO_3 photoelectrode. Large amount of anodic current was observed on the Ta_2O_5/RuO_2/FTO anode, although the current−potential curve was shifted slightly to the positive potential side. It is suggested that the water oxidation occurred through the Ta_2O_5 film also on the RuO_2/FTO anode.

Recently, it was reported that n-type semiconductor photoanodes such as Si, GaAs, and GaP for O_2 evolution were stabilized by overcoating with amorphous TiO_2 (4−143 nm thickness) prepared using atomic layer deposition,[23] although the valence band potential of TiO_2 was more positive than those of the n-type semiconductors. It is suggested that holes can transport across amorphous oxides independent of the valence band potentials. Moreover, it was found that the amorphous Ta_2O_5 film had small pores. We prepared Ta_2O_5, Nb_2O_5, and TiO_2 powder by the calcination of the same precursor solution used for the overcoated film. These powders were analyzed using a nitrogen adsorption−desorption measurement. The pore size and volume of the Ta_2O_5 was estimated as 1.7 nm and 0.002 mL g^{-1}, respectively, which were the smallest among these compounds (Table S1). In the case of amorphous Ta_2O_5-coated $BiVO_4$/WO_3 film with very small pores, it is surmised that the positive effect on the inhibition of the dissolution of the $BiVO_4$/WO_3 film was more preferential to the negative effect on the inhibition of transportation of holes, water, and O_2 by the amorphous and porous Ta_2O_5 overcoating.

CONCLUSIONS

To obtain enhanced stability with high photocurrent for a $BiVO_4$/WO_3 composite thin film photoelectrode, we performed a combinatorial study to discover new overcoating film materials and the optimum coating conditions on this composite photoelectrode using an automated semiconductor synthesis and screening system. Overcoating oxide film materials prepared using 13 different elements were examined with variation in the amounts of coated film. Among these overcoating oxide films, Ta_2O_5 calcined at 550 °C showed significant improvement in the stability of the $BiVO_4$/WO_3 photoelectrode in a highly concentrated bicarbonate electrolyte aqueous solution. This coated Ta_2O_5 film is amorphous and highly porous, and does not significantly diminish the photocurrent of the underlying $BiVO_4$/WO_3 photoelectrode nor inhibit the water oxidation reaction. The resulting protected photoelectrode material has significant potential for improved performance in water splitting applications. Furthermore, the loading of cocatalyst on photoanodes, which is one of the methods to improve both the efficiency and the stability, is under investigation.

ASSOCIATED CONTENT

Ⓢ Supporting Information

The Supporting Information is available free of charge on the ACS Publications website at DOI: 10.1021/acscombsci.5b00022.

> Illustrations of illumination positions and the photocurrents on the $BiVO_4$/WO_3/FTO substrate, comparative evaluation of the photocurrent of the multicomposite film samples, XRD spectra of the Ta_2O_5/$BiVO_4$/WO_3/FTO photoelectrode and Ta_2O_5 powder, linear sweep voltammograms of various electrodes, and physical properties of the Ta_2O_5, Nb_2O_5, and TiO_2 powders. (PDF)

AUTHOR INFORMATION

Corresponding Author

*E-mail: k.sayama@aist.go.jp

Notes

The authors declare no competing financial interest.

ACKNOWLEDGMENTS

The present work was partially supported by the Funding Program for Next Generation World-Leading Researchers (NEXT Program) from the Cabinet Office and by the Government of Japan and the Japan−U.S. Cooperation Project for Research and Standardization of Clean Energy Technologies.

REFERENCES

(1) Grätzel, M. Photoelectrochemical cells. *Nature* **2001**, *414*, 338−334.

(2) Cowan, A. J.; Durrant, J. R. Long-lived charge separated states in nanostructured semiconductor photoelectrodes for the production of solar fuels. *Chem. Soc. Rev.* **2013**, *42*, 2281−2293.

(3) Osterloh, F. E. Inorganic nanostructures for photoelectrochemical and photocatalytic water splitting. *Chem. Soc. Rev.* **2013**, *42*, 2294−2320.

(4) Sivula, K.; Le Formal, F.; Grätzel, M. Solar Water Splitting: Progress Using Hematite (α-Fe_2O_3) Photoelectrodes. *ChemSusChem* **2011**, *4*, 432−449.

(5) Park, Y.; McDonald, K. J.; Choi, K. S. Progress in bismuth vanadate photoanodes for use in solar water oxidation. *Chem. Soc. Rev.* **2013**, *42*, 2321−2337.

(6) Li, Z.; Luo, W.; Zhang, M.; Feng, J.; Zou, Z. Photoelectrochemical cells for solar hydrogen production: current state of promising photoelectrodes, methods to improve their properties, and outlook. *Energy Environ. Sci.* **2013**, *6*, 347−370.

(7) Liu, X.; Wang, F.; Wang, Q. Nanostructure-based WO_3 photoanodes for photoelectrochemical water splitting. *Phys. Chem. Chem. Phys.* **2012**, *14*, 7894−7911.

(8) Sayama, K.; Nomura, A.; Zou, Z.; Abe, R.; Abe, Y.; Arakawa, H. Photoelectrochemical decomposition of water on nanocrystalline $BiVO_4$ film electrodes under visible light. *Chem. Commun.* **2003**, *23*, 2908−2909.

(9) Sayama, K.; Wang, N.; Miseki, Y.; Kusama, H.; Onozawa-Komatsuzaki, N.; Sugihara, H. Effect of Carbonate Ions on the Photooxidation of Water over Porous $BiVO_4$ Film Photoelectrode under Visible Light. *Chem. Lett.* **2010**, *39*, 17−19.

(10) Saito, R.; Miseki, Y.; Sayama, K. Highly efficient photoelectrochemical water splitting using a thin film photoanode of $BiVO_4$/SnO_2/WO_3 multi-composite in a carbonate electrolyte. *Chem. Commun.* **2012**, *48*, 3833−3835.

(11) Saito, R.; Miseki, Y.; Sayama, K. Photoanode characteristics of multi-layer composite $BiVO_4$ thin film in a concentrated carbonate

electrolyte solution for water splitting. *J. Photochem. Photobiol., A* **2013**, *258*, 51−60.

(12) Fujimoto, I.; Wang, N.; Saito, R.; Miseki, Y.; Gunji, T.; Sayama, K. WO_3/$BiVO_4$ composite photoelectrode prepared by improved auto-combustion method for highly efficient water splitting. *Int. J. Hydrogen Energy* **2014**, *39*, 2454−2461.

(13) Sayama, K.; Nomura, A.; Arai, T.; Sugita, T.; Abe, R.; Yanagida, M.; Oi, T.; Iwasaki, Y.; Abe, Y.; Sugihara, H. Photoelectrochemical Decomposition of Water into H_2 and O_2 on Porous $BiVO_4$ Thin-Film Electrodes under Visible Light and Significant Effect of Ag Ion Treatment. *J. Phys. Chem. B* **2006**, *110*, 11352−11360.

(14) Seabold, J. A.; Choi, K. S. Efficient and stable Photo-Oxidation of Water by a Bismuth Vanadate Photoanode Coupled with an Iron Oxyhydroxide Oxygen Evolution Catalyst. *J. Am. Chem. Soc.* **2012**, *134*, 2186−2192.

(15) Zhong, D. K.; Choi, S.; Gamelin, D. R. Near-Complete Suppression of surface Recombination in Solar Photoelectrolysis by "Co-Pi" Catalyst-Modified W:$BiVO_4$. *J. Am. Chem. Soc.* **2011**, *133*, 18370−18377.

(16) Luo, W.; Yang, Z.; Li, Z.; Zhang, J.; Liu, J.; Zhao, Z.; Wang, Z.; Yan, S.; Yu, T.; Zou, Z. Solar Hydrogen Generation from Seawater with a Modified $BiVO_4$ Photoanode. *Energy Environ. Sci.* **2011**, *4*, 4046−4051.

(17) Arai, T.; Konishi, Y.; Iwasaki, Y.; Sugihara, H.; Sayama, K. High-Throughput Screening Using Porous Photoelectrode for the Development of Visible-Light-Responsive Semiconductors. *J. Comb. Chem.* **2007**, *9*, 574−581.

(18) Kusama, H.; Wang, N.; Miseki, Y.; Sayama, K. Combinatorial Search for Iron/Titanium-Based Ternary Oxides with a Visible-Light Response. *J. Comb. Chem.* **2010**, *12*, 356−362.

(19) Matsui, Y.; Hiratani, M.; Kimura, S.; Asano, I. Combining Ta_2O_5 and Nb_2O_5 in Bilayered Structures and Solid Solutions for Use in MIM Capacitors. *J. Electrochem. Soc.* **2005**, *152*, F54−F59.

(20) Hong, S. J.; Lee, S.; Jang, J. S.; Lee, J. S. Heterojunction $BiVO_4$/WO_3 electrodes for enhanced photoactivity of water oxidation. *Energy Environ. Sci.* **2011**, *4*, 1781−1787.

(21) Xu, Y.; Schoonen, M. A. A. The absolute energy positions of conduction and valence bands of selected semiconducting minerals. *Am. Mineral.* **2000**, *85*, 543−556.

(22) Lyons, M. E. G.; Floquet, S. Mechanism of oxygen reactions at porous oxide electrodes. Part 2—Oxygen evolution at RuO_2, IrO_2 and $Ir_xRu_{1-x}O_2$ electrodes in aqueous acid and alkaline solution. *Phys. Chem. Chem. Phys.* **2011**, *13*, 5314−5335.

(23) Hu, S.; Shaner, M. R.; Beardslee, J. A.; Lichterman, M.; Brunschwig, B. S.; Lewis, N. S. Amorphous TiO_2 coatings stabilize Si, GaAs, and GaP photoanodes for efficient water oxidation. *Science* **2014**, *344*, 1005−1009.